Modeling nearshore sediment transport along the Canadian Beaufort Sea coast

Md. Azharul Hoque
Geological Survey of Canada (Atlantic), Natural Resources Canada
1 Challenger Drive, Dartmouth, Nova Scotia, B2Y 4A2, Canada

Steven M. Solomon
Geological Survey of Canada (Atlantic), Natural Resources Canada
1 Challenger Drive, Dartmouth, Nova Scotia, B2Y 4A2, Canada

William Perrie
Fisheries and Oceans Canada
1 Challenger Drive, Dartmouth, Nova Scotia, B2Y 4A2, Canada

ABSTRACT
We have studied the temporal and spatial variability of wave energy and sediment transport along the Beaufort Sea nearshore using a 21-year (1985-2005) hourly wave hindcast dataset. The highest energy and longshore transport in this region occurs along the Yukon coastline, followed by Tuktoyaktuk peninsula. Temporal variations show large year-to-year variability. Substantial transports are found in 1985, 1993, 1999 and 2005. Although longshore transports are dominated by westerly and northwesterly storm waves, easterly transport has been increasing in recent years.

RÉSUMÉ
Nous étudions la variabilité temporelle et spatiale de l'énergie des vagues et du transport de sédiments le long de la zone littorale de la mer de Beaufort, à l'aide d'un jeu de données de prévisions horaires *a posteriori* des vagues sur une période de 21 ans (de 1985 à 2005). L'énergie des vagues et le transport de sédiments sont les plus importants d'abord le long de la côte du Yukon et en deuxième lieu le long de la péninsule de Tuktoyaktuk. Les variations temporelles indiquent une grande variabilité d'une année à l'autre. Des transports importants ont eu lieu au cours des années 1985, 1993, 1999 et 2005. Bien que les transports de sédiments le long du littoral soient dominés par des ondes de tempête de l'ouest et du nord-ouest, les transports depuis l'est ont augmenté au cours des dernières années.

1 INTRODUCTION

Nearshore hydrodynamics and their impacts on the coast and seabed are concerns for hydrocarbon exploration and development in the Beaufort Sea. Development scenarios under consideration include increased ship and barge traffic, potential dredging to improve access to facilities and exploration areas, pipelines and artificial island construction. Movement of sediment will directly affect these activities through possible adverse environmental impacts related to construction and increased project costs. Coastal erosion and associated changes in nearshore ecology also have the potential to directly affect local communities since hunting, fishing and trapping are economic and cultural mainstays for many aboriginal communities. Numerous historical and archaeological sites in the region are threatened by coastal retreat.

Climate change in the Arctic will have profound impacts on the permafrost coastline of Canada's Beauport Sea. Lambert (1995) suggested an increase in the frequency of severe high latitude storms under global warming. Solomon et al. (1994) reported that there is a strong correlation between storm intensity and coastal erosion along the Beaufort Sea. Thirty kilometres seaward of the Mackenzie River Delta, water depths are less than five metres. These shallow depths and low gradients present a variety of challenges for data collection and modeling. Long ice-free fetches during the open water season can cause large waves and high storm surges to propagate towards this area with associated impacts on the coast (Solomon and Covill 1995). During the open water season, storms generate waves and currents which play a strong role in coastal erosion and shoreline changes. The coast of the Beauport Sea is micro-tidal with astronomical tides less than 0.5m, so coastal sediment transports are wave dominated particularly during the open water period.

Previous works mostly considered specific storm generated waves (i.e. Solomon and Covill 1995, Héquette and Barnes 1990, Héquette and Hill 1993, 1995, Héquette et al. 2001) or short term offshore wave climate (Couture et al. 2008) in their evolution of erosion in this region. Hequette et al. (1993, 2001) studied storm-generated shoreface sediment transport based on wind, waves and current measurement at two coastal sites. However, they only considered the area seaward of the surf zone and were not concerned with sediment transport in the surf zone which is dominated by the longshore current and energy from breaking waves. Solomon (2005) reported that coastal retreat in the Mackenzie region of the Canadian Beaufort Sea is 0.6 m/ year on average, and can range as high as 22.5 m/ year. The dominant cliff retreat processes along the coast of Canadian Beaufort Sea are: thermo-erosion during storms, block failure and retrogressive thaw slump. In cases of block failures and retrogressive thaw slumps sediment is mostly deposited close to the water line or in

the swash zone and surf zone. The erosion of the sediment from such failures may not occur immediately thus protecting the shoreline and cliffs for a while. This ice-rich material is potentially subjected to longshore transport by even moderate wave action. Once this material is removed, the toe of the bluff is not longer protected from direct wave action and subsequent shoreline retreat proceeds. Thus, wave energy and longshore sediment transport gradients substantially control the morphological changes in this region.

The main goal of this paper is to evaluate the long-term nearshore sediment transport based on a 21 (1985-2005) year wave hindcast data set of the Beaufort Sea. Our specific objectives are:

(i) to study the wave energy profile along the coast,
(ii) to calculate the longshore sediment transport using the energy flux.

2 STUDY AREA

This study covers the coastline along the Canadian Beaufort Sea (Figure 1). The Beaufort Sea is the southward extension of the Arctic Ocean and occupies an area of approximately 450,000 km^2. The continental self slopes gently to the shelf break located at about 80 m water depth (Hill et al. 1991). The shelf is relatively narrow, ranging from 40 km wide in the western portion of this area to over 150 km wide off the Mackenzie Delta.

Much of the sea is permanently covered by the polar ice pack. However, there is a portion of the sea in the south that does become ice-free during the summer, typically late June until mid-October. During this time storms can have a notable impact because the extent of open water is maximal. Storm winds, which become increasingly frequent in late August and September, come predominantly out of the west and northwest and occur during the period of the greatest open water extent and prior to the initiation of freeze-up (Solomon 2005).Thus, the largest waves and highest storm surges of the season occur just before the Beaufort Sea freezes over (Hudak and Young 2002).

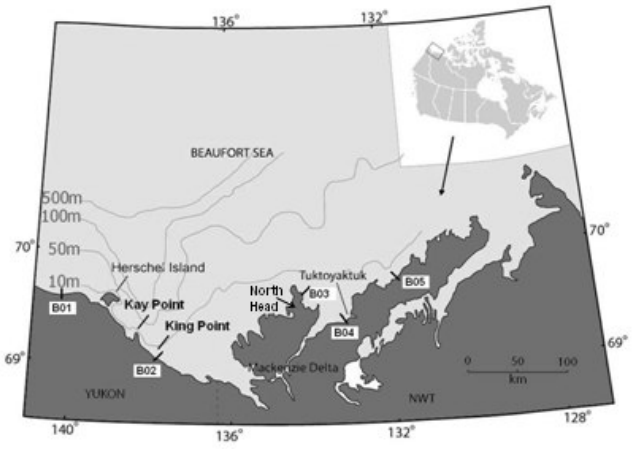

Figure 1. Study area showing the locations of sediment transport calculations.

Table 1. Nearshore wave hindcast locations, water depth and bottom slope at the five transects in Figure 1.

Transect	Wave hindcast location		Water depth (m)	Bottom slope down to 5m water depth
	Longitude (deg)	Latitude (deg)		
B01	-140.25	69.60	18.50	0.70
B02	-138.00	69.15	24.00	0.89
B03	-134.10	69.70	5.00	0.02
B04	-133.20	69.50	5.00	0.02
B05	-132.00	69.85	7.73	0.18

Five transects with varying profile and shoreline orientations along the coast of Canadian Beaufort Sea are selected: two (B01 and B02) on the Yukon coastal plain, one (B03) on the NE coast of North Head and two (B03 and B0) on the coastline of Tuktoyaktuk peninsula. Output locations of hindcasted wave parameters, water depth and bottom slope are shown in Table 1.

3. STUDY METHODS

3.1 Wave Hindcasting and Transformation

Wave energy and associated longshore transport along the coastline of the Beaufort Sea are calculated using the long-term (1985-2005) wave hindcast of Environment Canada's Meteorological Service of Canada Beaufort (MSCB) project. In that project Swail et al. (2007) produced hourly wave hindcast for 1985-2005, denoted hereafter as MSCB. The wave model applied in MSCB was the third generation wave model (OWI-3G) used in the original AES40/MSC50 hindcast (see Swail et al. 2006 for the description of the model). Boundary spectra along the southern boundary of the basin model were supplied from the GROW (Global Reanalysis of Ocean Waves) hindcast which applied a 2nd generation wave model on a global grid (Cox and Swail 2001). A fine resolution (0.05° in the north-south direction and 0.15° in the east-west) was inscribed in the Beaufort coarse grid (28km) model. This fine resolution regional grid represents 3442 active grid points. The time series of hindcasted wave heights H_s and peak periods T_p at MSCB grid points nearest to the shorelines at study locations are used as wave inputs in the present analysis.

Water depths at MSCB nearshore locations are 5m or more and hindcasted waves are mostly deep water waves (d/L>0.5, where d is water depth and L is wave length). According to small amplitude wave theory, wavelength is expressed as

$$L = \frac{gT^2}{2\pi}\tanh(kd) \qquad [1]$$

where k is wave number ($2\pi/L$), and d is water depth.

As waves approach the shore, the bottom of a wave begins to interact with the seabed and shoaling occurs. The shoreline and depth contour at the selected transects

are relatively straight and parallel. Wave shoaling and transformations are calculated using the simple approaches of linear wave theory transformations (Smith 2002; Kamphuis 2000). Refraction and shoaling of incident linear waves are calculated using Snell's law and the conservation of wave energy flux. If K_s is the shoaling coefficient and K_r is the refraction coefficient, wave height H at any depth can be related to deep water wave height H_0 as:

$$H = H_0 * K_r * K_s \quad [2]$$

Using conservation of energy propagation, the shoaling coefficient (K_s) that relates wave height at any water depth to deep water wave height is expressed as:

$$K_s = \sqrt{\frac{n_0 C_0}{nC}} \quad [3]$$

where C is the velocity of propagation of individual waves, n is the group velocity parameter, and the subscript '*0*' indicates offshore waves.

When waves approach the shore at an angle, wave refraction takes place, in which the wave crests bend to align themselves with the bottom contours and the wave direction becomes more perpendicular to shore. In the simple wave refraction calculation, the propagation equation is simplified to Snell's Law and the refraction coefficient is expressed (Kamphuis, 2000) as:

$$K_r = \sqrt{\frac{\cos\alpha_0}{\cos\alpha}} \quad [4]$$

where α is the wave incident angle with the direction normal to the shoreline, and the subscript '0' indicates the offshore incident angle. Following Snell's Law of wave refraction the expression relating the wave incident angles can be written as:

$$\frac{\sin\alpha}{\sin\alpha_0} = \frac{C}{C_0} \ . \quad [5]$$

The shallow water wave breaking criterion defines wave parameters at the breaking point. The wave breaking criteria used in the present analysis is based on the wave theory criterion for single waves (McCowan 1894, Munk 1949) as H_b/d_b=0.78 (where, H_b and d_b represent significant wave height and water depth at breaking).

3.2 Wave Energy and Longshore Transport

Longshore sediment transport is related to the wave - generated momentum or energy gradient. Wave energy is calculated based on the following equation:

$$E = \rho g H^2 / 8 \quad [6]$$

where E is wave energy per unit area (N/m^2), H_s is significant wave height and g the acceleration due to gravity.

The energy flux per unit width of wave crest is given as ECn, where C is the wave celerity (C=L/T). The longshore component of wave energy flux is given as:

$$P_l = (ECn)_b \sin\alpha_b \cos\alpha_b \quad [7]$$

where $(ECn)_b$ is the wave energy flux (per unit length of shoreline) when breaking occurs.

The equation for the bulk sediment transport rate is given by the Shore Protection Manual (CERC, 1984) as:

$$I_s = KP_l \quad [8]$$

where I_s is the immersed weight of sediment transported having the same unit as P_l (i.e. N/sec or lbf/sec), and K is a dimensionless co-efficient of proportionality.

Several laboratories and field studies have been carried out to determine the value of K. Komar and Inman (1970) introduce a K coefficient as 0.77 assembling the different laboratory and field data. Bailard (1981, 1984) developed an energy-based model, which represents K as a function of the breaker angle and the ratio of orbital velocity magnitude and sediment fall speed, also based on the rms wave height at breaking. The Shore Protection Manual (CERC 1984) presents the value of K as 0.39 based on computation using the significant wave heights.

If the density and porosity of sediment particles are ρ_s and p, the volume transport rate is:

$$Q = \frac{KP_l}{(\rho_s - \rho)(1-p)} \quad [9]$$

Equations (8) and (9) give the total littoral transport, which consists of the suspended load and the bed load. The longshore sediment flux at different study locations is calculated using Equation 9 and applying the wave heights and wave incident angles at breaking, which are obtained through the wave shoaling calculation as discussed earlier in this section. As there is no calibrated value of K for this region, we assume the K value is 0.39 (recommended by CERC (1984) for significant wave heights) for model calculations. The values of other parameters used in sediment transport computations are: ρ_s=2650 kg/m^3, ρ=1025 for salt water, g=9.81 m/s^2, and p=0.3. Longshore transport is considered positive when the sediment transport is to the right of an observer looking out to the sea.

4. RESULTS AND DISCUSSIONS

For our study points, the nearshore wave roses are shown in Figure 2, based on hourly wave hindcast during 1985-2005 for open water (July-Sept) seasons. Waves are predominantly from the northwest, north and northeast directions.

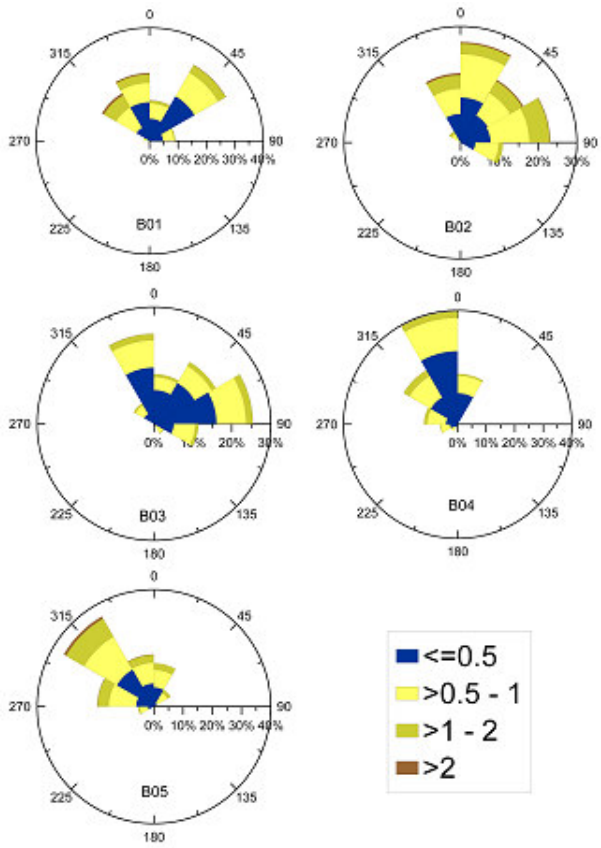

Figure 2. Nearshore wave roses showing frequency distributions at five study locations computed from MSCB hindcast waves during 1985-2005.

The longshore transport profiles for the period 1985-2005 (as discussed later in this section) illustrate the pattern of temporal and spatial variations of wave energy along the coast of the Canadian Beaufort Sea. The coastline at B01 is subjected to highest wave energy followed by the coastline at King point (which represents the region from Herschel Island to Mackenzie delta) and Tuktoyaktuk peninsula (as represented by location B05). The causes of such energy variations are shoreline orientations, wind directions, open water fetch, wave intensities and shoreface bathymetry. During the open water season most of the high energy waves are predominantly from the west and northwest directions (Hequette et al. 2001, Hoque et al. 2009). The shoreline at B01 and B05 are subjected to wave energy from all three dominant directions (northwest, north and northeast). However, the shorelines facing the northeast direction (B02, B04) are subjected to substantial wave energy from the northeast and east.

Another important cause of wave energy gradients is likely the refraction and dissipation processes that the deep water waves encounter as they approach the coast. The portion of the Beaufort shelf facing the Mackenzie Delta and eastward is much wider with very mild bottom slopes (≤0.01). Therefore the wave transformation and dissipation processes act for a longer time and by the time the waves arrive at the coast and break, a large amount of energy has already been lost. In contrast along the Yukon coastal plain, the shoreface is narrower and steeper so that the refraction and dissipation processes are less effective and the wave do not lose as much energy before they break. Hence this region is subjected to higher wave energy than the regions to the east.

The transect B01, which represents the western Yukon coastline is subjected to higher wave energy from westerly and northwesterly storms resulting in mostly positive (in this case easterly) longshore transport. However the wave energy due to easterly winds is found to be dominant in 1997 and 2005 resulting higher longshore transport to the leftward (-ve) direction. Throughout the computation duration (1985-2005) the net transport in this location is found to be in the positive direction and 28.58×10^3 m^3/year (Table 2) thus resulting in depositional gradients along the coastline eastward from Komakuk beach. This is consistent with the development and maintenance of an extensive barrier spit and island complex east of Transect B01.

The four severe storm-generated wave events during the MSCB hindcast duration (1985-2005) occurred in 1985, 1993, 1999 and 2000; and nearshore waves were predominantly from the northwest direction during all these storms (Hoque et al. 2009). However the wave intensities in the nearshore region are substantially lower during 2000 storm compared to the other three storms, due to the extensive ice cover in the Beaufort Sea at that time. High rates of positive transport in 1985, 1993 and 1999 (as shown in Figure 3) are the effects of severe storm events in those years.

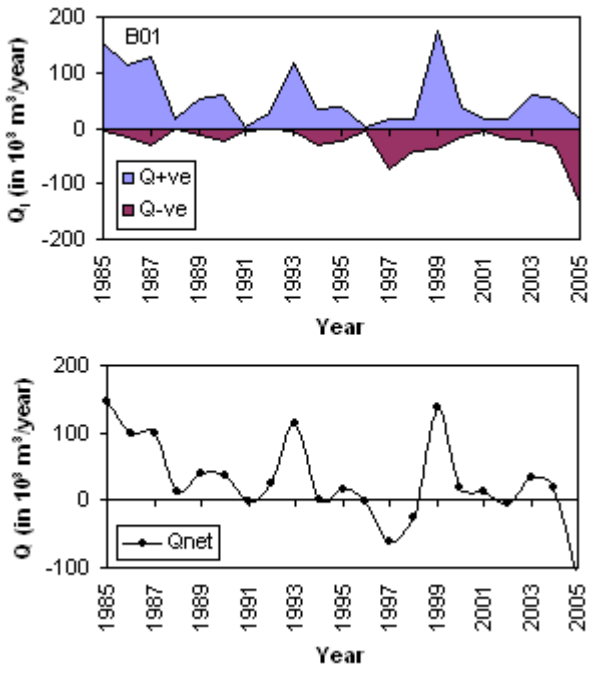

Figure 3. Longshore sediment transport at Transect B01.

Table 2. Yearly averaged longshore transport rates during the computation duration (1985-2005).

Transect	Q_{+ve} (rightward) (10^3 m^3/year)	Q_{-ve} (leftward) (10^3 m^3/year)	Q_{net} (10^3 m^3/year)
B01	54.38	-25.80	28.58
B02	39.49	-31.36	8.14
B03	14.65	-17.9	-3.25
B04	4.04	-15.41	-11.37
B05	27.0	-21.50	5.50

Transect B02 at King Point is sheltered from severe westerly wave attacks as the coastline is concave and faces the northeast direction. However this location is still subjected to strong wave energy from both northwest and east directions, resulting in substantial longshore transport (Figure 4). Among the three major wave events in 1985, 1993 and 1999, this location is found be well sheltered in the 1985 and 1993 storms and subjected to the highest positive (rightward) longshore sediment transport in the 1999 storm event. The peak positive transports are due to westerly and northwesterly storm events (as shown in top panel of Figure 5 for the year 1999). The leftward (or westerly) transports at B01 and B02 have been found to have increased in the last few years of the computational period showing a substantial negative transport in 2005, which is due to longer duration moderate easterly waves in September 2005 (bottom panel of Figure 5). Long-term positive (easterly) transport is consistent with morphological changes along this coast documented by Hill (1990). The longshore transport rates at B01 and B02 are higher compared to the eastern portion of the Canadian Beaufort Sea coast (Table 2)

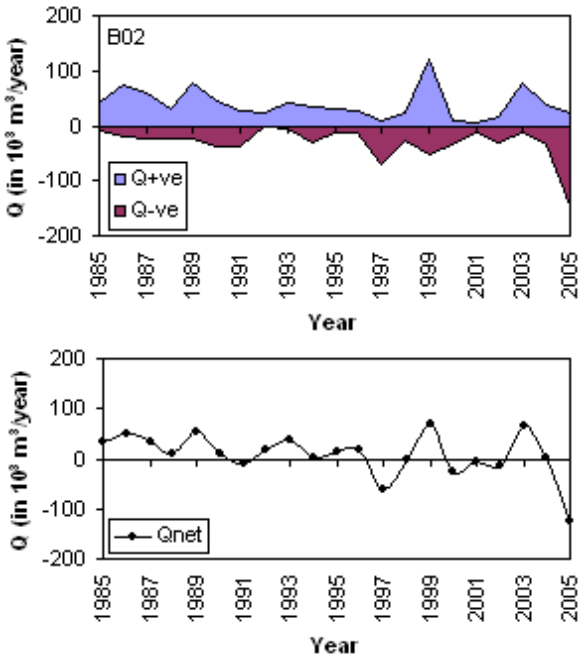

Figure 4. Longshore sediment transport at Transect B02.

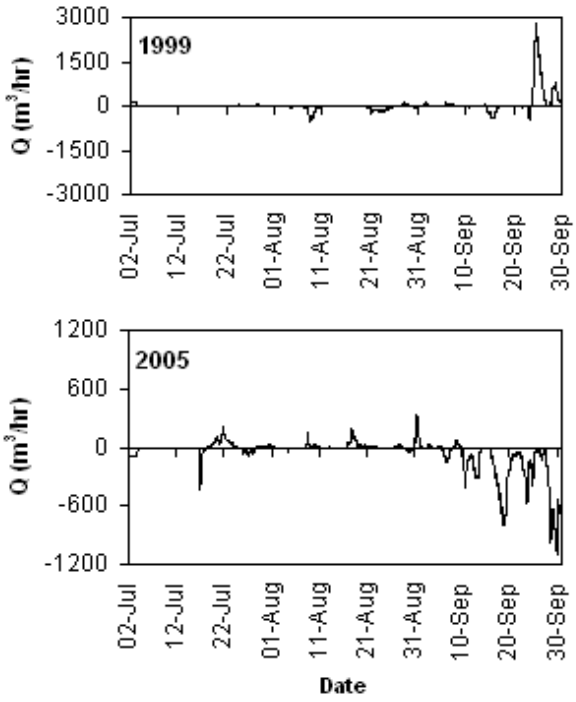

Figure 5. Temporal distribution of hourly longshore transport at Transect B02 in 1999 and 2005 showing the influence of a major events in 1999 versus multiple moderate events in 2005.

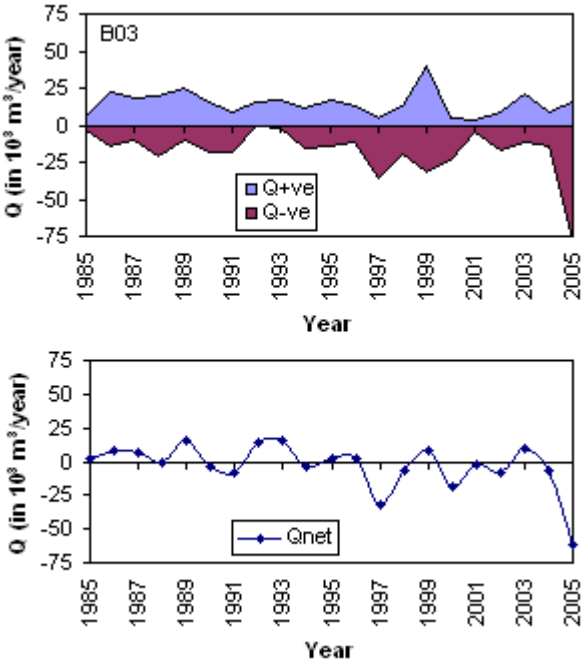

Figure 6. Longshore sediment transport at Transect B03 (Note: Y-axis scale is different than preceding diagrams).

The shoreline at B03 faces NE and it seems to be sheltered from westerly whereas due to wave refraction and shoaling, waves from the north and NNW directions can generate positive longshore currents in this area thus causing positive longshore transport. Although waves generated by strong winds from the east and southeast are not very large due to limited fetch, even these moderate waves cause substantial longshore transport as shown in Figure 6 and Table 2. The average net transport across transect B03 is -3.25 x10^3 m^3/year (Table 2).

Although the yearly averaged potential longshore transport at B03 is found to be in the leftward (negative) direction, but orientation of spits and barrier beaches (Figure 7) in this region suggests that long-term net wave energy gradient and associated longshore transport would be to the rightward (positive) direction. Based on storm generated waves which are predominantly from the northwest direction (Hoque et al. 2009), the trend of longshore transport at this location would be positive as obtained for the cases of B02.

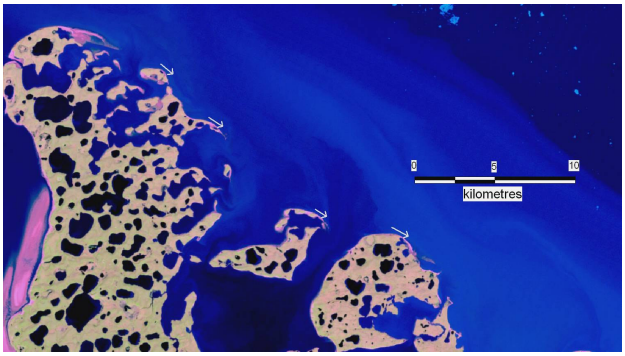

Figure 7. Landsat imagery of the eastward facing coastline of North Head in the region represented by transect B03. Arrows depict the direction of long-term net sediment transport based on orientation of spits and barrier beaches.

The net transport over the computation period 1985-2005 would actually be positive (rightward). But due to a large amount of negative transport in September 2005 (Figure 8), the net transport is found potentially to be in the negative (leftward) direction. If we exclude Sept 2005 transport the total yearly averaged net transport would be 305 m^3/year to the rightward direction. But if we include the Sept 2005 transport the scenario is totally opposite; and a large volume of longshore transport -3247 m^3/year is found to the leftward direction. As discussed earlier, the peak positive transports are found to be due to westerly and northwesterly storms. There was no severe storm in Sept 2005. But, as illustrated in Figure 9, moderate and persistent easterly waves (with maximum wave heights close to 2 m) for a longer duration causes large amount of potential leftward transport in Sept 2005.

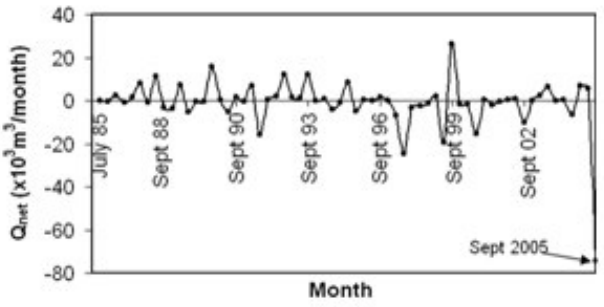

Figure 8. Monthly averaged longshore transport at Transect B4 during 1985-2001.

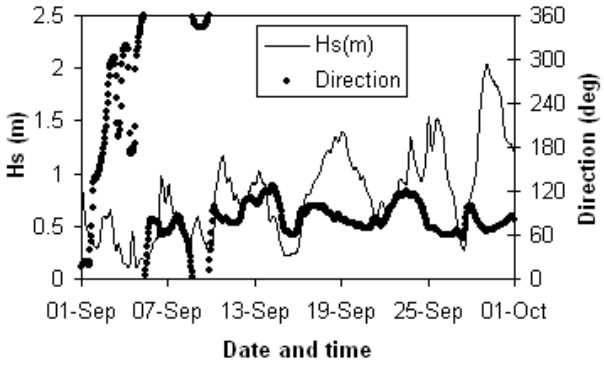

Figure 9. Hourly significant wave heights and incoming wave direction (clockwise positive from north) in September 2005 at the nearshore MSCB location on transect B03.

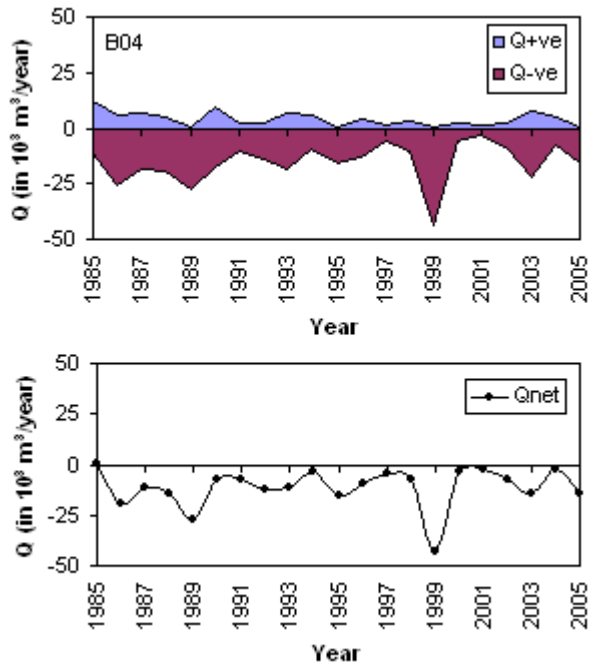

Figure 10. Longshore sediment flux at Transect B04. (Note: Y-axis scale is different than preceding diagrams).

The longshore sediment transport along the coastline of the Tuktoyaktuk peninsula is studied at two transects (B04 and B05). Transect B04 is located at the Tibjak Beach north of Tuktoyaktuk and the coastline faces WNW. It is well sheltered from the easterly storms and somewhat sheltered to the west. As illustrated in Figure 9, computed potential longshore transports are found to be higher to the leftward direction (-15.41x10^3 m^3/year) compared to that to rightward direction (4.04 x10^3 m^3/year) (Table 2). This is due to the reason that this transect is subjected to longshore energy flux from the NW, N and NE, which contribute to the leftward transport at this transect. The westerly waves result in less significant affect, which is in agreement with Hequette (1993). Positive transports (Figure 10) might be mainly due to fetch-limited wind generated waves in the bay.

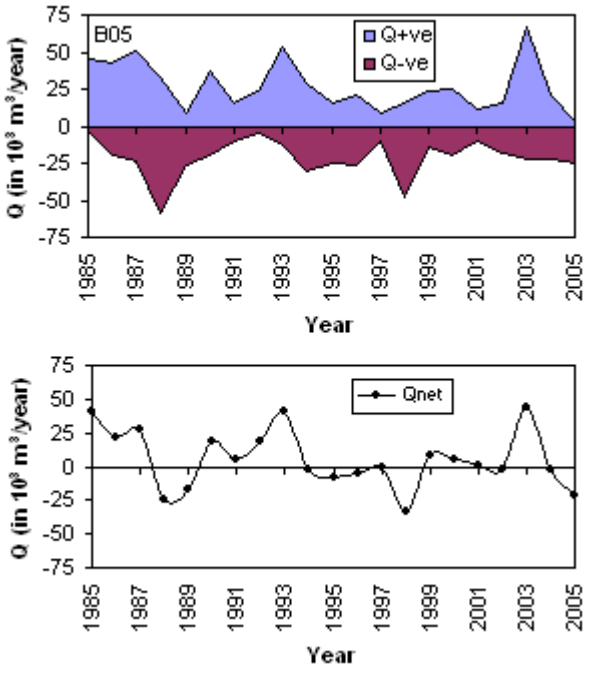

Figure 11. Longshore sediment transport at Transect B05.

The shoreline at transect B05 faces NW and is subjected to most of the severe wave attacks with positive longshore transport of 27 x10^3 m^3/year. This location also shows substantial negative longshore transport (-21x10^3 m^3/year) potential. The waves from north and northeast direction contribute to leftward transport. However, the high rates of longshore transport in both directions throughout the study period would be the result of westerly and northwesterly storm. Slight variations in the direction of westerly and northwesterly storm directions would result in variations in potential longshore transport directions and magnitude. Net potential transport at B05 is 5.5x10^3 m^3/year (reported in Table 2). The bimodal nature of transport here is illustrated by the large flaking splits emanating from headlands (Figure 12). There are low barriers that are easily submerged and over washed (Héquette et al. (2001). Such processes, will affects the wave energy profile and associated longshore transport.

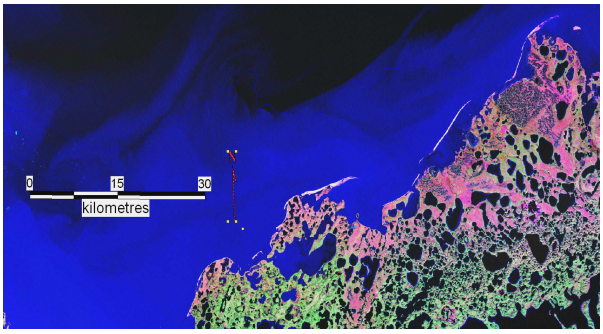

Figure 12. Coastline adjacent to the study location B05 in Tuktoyaktuk peninsula.

The shoreline orientations along the coasts of north Head and Tuktoyaktuk Peninsula show high spatial variability (Figure 10 and 12). Such a variation of shoreline planform orientations influences the potential longshore transport both in magnitude and direction. The existence of spits along these coasts suggests spatial variations of longshore sediment transport. Computation of potential longshore transport at finer space grids will clarify the influence of shoreline orientation. The work of Héquette et al. (2001) also reported that coastal morphology may play a significant role on circulation and sediment transport on the shoreface.

5. CONCLUSIONS

This study presents analyses of wave energy and associated potential longshore transport based on hourly wave hindcast for 21 years (1985-2005). Computational results draw the following conclusions:

(i) Temporal variations show that year-to-year variability is quite large, with some years (especially those with identified severe storm events such as 1985, 1993, 1999) experiencing high wave energy and large amount of alongshore transports.

(ii) The spatial variability of five studied locations clearly indicate a distinct east-west trend. The Yukon coastline is subject to higher longshore wave energy fluxes and associated longshore transports compared to the eastern portion of the Canadian Beaufort Sea coastline. As the shoreface slopes at B01 and B02 are very steep, most waves break close to the cliffs and cliff retreat due to thermo-erosion and block failures are the source of sediment supply

(iii) The net yearly average longshore transports over the computational duration (1985-2005) are in the positive directions at transects B01, B02, and B05; and in the negative directions at transects at B04.

(iv) Potential net longshore transport at Transect B03 (which represents the NE coastline of the North Head) is found to be leftward, which is due to the large

amount of leftward sediment transport caused by moderate easterly wave actions for a longer period of time in September 2005.

(v) Shorelines facing northeast exhibit an increasing rate of negative longshore energy flux and sediment transport in recent years with highest negative transports in 2005. This finding clearly indicates the increasing role of easterly storms in longshore transport.

Our analysis covers model-based computations of temporal and spatial variability of wave energy flux and potential longshore transport along the coast of the Canadian Beaufort Sea. The analysis in this paper used the well known transport model derived by CERC (1984) based on different field data sets and is widely used for engineering applications. Moreover a data base of 21 years of fine-resolution wave hindcast is used as inputs to examine long-term spatial and temporal variations of wave energy and potential longshore transport rates. Finding of the present study have implications for planning future development and sediment management in this region. In ongoing research, our objective is to improve the understanding of storm-generated cliff retreat, cross-shore and longshore transport, impacts of long-period easterly waves in September 2005, potential long-term morphodynamics and effects of climate change.

ACKNOWLEDGEMENTS

This paper is Geological Survey of Canada Contribution no 20080634. Support for this research comes from the Canadian Panel on Energy Research and Development (PERD-Offshore Environmental Factors and Northern Programs), and the Canadian Federal IPY Office.

REFERENCES

Bailard, J.A. 1981. An energetics total load sediment transport model for a plain sloping beach. *Journal of Geophysical Research*, 86C(11):10938-10954.

Bailard, J.A. 1984. A Simplified model for longshore sediment transport. *Proc. 19th Int. Coastal Engg. Conf. 1994*, ASCE, New York, 1454-1470.

CERC (Coastal Engineering Research Center), 1984. *Shore protection manual.* U.S. Army Corps of Engineers, Vicksburg, Mississippi, USA.

Cox, A.T., and V.R. Swail, 2001. A global wave hindcast over the period 1958-1997: validation and climate assessment. *Journal of Geophysical Research* 106C(2): 2313-2329.

Héquette, A. and Barnes, P.W. 1990. Coastal retreat and shoreface profile variations in the Canadian Beaufort Sea. *Marine Geology*, 91: 113-132.

Héquette, A. and Hill, P.R. 1993. Storm generated currents and offshore sediment transport on a sandy shoreface, Tibjak Beach, Canadian Beaufort Sea, *Marine Geology*, 113: 283-304.

Héquette, A. and Hill, P.R. 1995. Response of the seabed to storm-generated combined flows on a sandy Arctic shoreface,Canadian Beaufort Sea. *Journal of Sedimentary Research*, A65(3): 461-471.

Hequette, A., Desrosiers, M., Hill, P.R. and Forbes, D.L. 2001. The influence of coastal morphology on shoreface sediment transport under storm-combined flows, Canadian Beaufort Sea. *Journal of Coastal Research*, 17(3):507-516.

Hill, P.R., 1991. Coastal geology of thr King Point area, Yukon Territory, Canada. Marine Geology, 91: 93-111.

Hill, P.R., Blasco, S.M., Harper, J.R. and Fissel, D.B. 1991. Sedimentation on the Canadian Beaufort Self. *Continental Self Research* 11, 821-842.

Hoque, M.A., Solomon, S. and Perrie, W. 2009. Nearshore waves in the southern Beaufort Sea during severe Arctic storms. *Proc. 20th Int. Con. on Port and Ocean Engg. under Arctic Conditions* 2009, Lulea, Sweden. (in press)

Hudak, D.R. and Young, M.C., 2002. Storm climatology of the southern Beaufort Sea. *Atmosphere-Ocean*. 40 (2), 145-158.

Lambert, S.J. 1995. The effects of enhance greenhouse warming on winter cyclone frequencies and strength. *Journal of Climate*, 8:1447-1452.

Kamphuis, J.W., 2000. *Introduction to coastal engineering and management*. World Scientific, Singapore, 437p.

Komar, P.D. and Inman, D.L. 1970. Longshore sand transport on beaches, Journal of Geophysical Research, 75(30) 5914-5927.

Couture, N., Hoque, M.A**.** and Pollard, W.H., 2008. Modeling the erosion of ice-rich deposits along the Yukon Coastal Plain. *Proc. 9th Int. Permafrost Conference 2008,* Alaska, 303-308.

Smith, J.M., 2002. Surf zone hydrodynamics, In: Vincent, L., and Demirbilek, Z. (ed.), *Coastal Engineering Manual*, *Part II, Hydrodynamics, Chapter II-2,* Engineer Manual 1110-2-1100, U.S. Army Corps of Engineers, Washington, DC, USA.

Solomon, S.M. Forbes, D.L. and Keirstead, B. 1994. *Coastal impact of climate change: Beaufort Sea erosion study*, Open file 2890, Geological Survey of Canada.

Solomon S.M. and Covill R., 1995. Impacts of the September 1993 Storm on the Beaufort Sea. *Proc. 7th Canadian Coastal Conf.1995, Halifax, NS, Canada,* 2:779-795.

Solomon, S.M. 2005. Spatial and temporal variability of shoreline change in the Beaufort-Mackenzie region, Northwest Territories, Canada. *Geo-marine Letters* 25: 127-137.

Swail, V.R., Cardone, V.J., Ferguson, M., Gummer, D.J. and Cox, A.T., 2007. MSC Beaufort Sea wind and wave reanalysis, *10th Int. Wind and Wave Workshop*, 2007, Oahu, Hawaii.